N08500108

UNIVERSITY OF OSLO

INSTITUTE OF PHYSICS REPORT SERIES

ISSN 0332-5571

ON THE SHORT-DISTANCE DOUBLE PENGUIN CONTRIBUTION TO THE K^0-$\overline{K^0}$ MIXING

J.O. Eeg
Institute of Physics, University of Oslo
Oslo, Norway
I. Picek
Rudjer Bošković Institute, Zagreb, Croatia
Yugoslavia

Report 85-06 Received: 25.04-1985

ON THE SHORT-DISTANCE DOUBLE PENGUIN CONTRIBUTION TO THE K^0-$\overline{K^0}$ MIXING

J.O. Eeg
Institute of Physics, University of Oslo,
Oslo, Norway

I. Picek
Rudjer Bošković Institute, Zagreb, Croatia,
Yugoslavia

We investigate the short-distance contribution of the double penguin box diagram to the K^0-$\overline{K^0}$ mixing. Compared with previous work of other authors, the present paper takes into account (i) the momentum dependence of the box loop, (ii) both the non-local part of the penguin and the previously considered local part and (iii) the crossed diagrams, which make a class of double penguin diagrams complete. With such new ingredients, we arrive at the conclusion that the SD part of the double penguin is physically irrelevant. After eliminating this particular mechanism for the K^0-$\overline{K^0}$ mixing, we point out other potentially relevant mechanisms.

1. Introduction. The very small value of the K^o-$\overline{K^o}$ transition amplitude was accounted for by the Glashow-Iliopoulos-Maiani (GIM) mechanism |1| in the lagrangian at the tree level. The related K_L-K_S mass difference calculated in terms of quark fields exhibited that the GIM mechanism also operates at the one-loop level |2|. In turn, such a calculation made possible the quantitative estimate of the charmed-quark mass. This is due to the explicit appearance of m_c^2 in the local short-distance (SD) effective lagrangian of the K^o-$\overline{K^o}$ transition, calculated for two generations of quarks. In the evaluation of the simple box diagram, inclusion of the third generation results in the K^o-$\overline{K^o}$ transition matrix |3,4| which also contains the imaginary CP-violating part.

A recent extraction of a bound on the top-quark mass by Hochenberg and Sachs |5| relied on another type of box diagram, the double penguin box (fig. 1a). Hochenberg and Sachs argued that the double penguin box led to the local SD lagrangian proportional to m_t^2, which enabled them to derive the bound $m_t < 45$ GeV. In contrast to this local SD treatment of the double penguin, the original |6| and recent |7| treatments of the double penguin focused on the long-distance (LD) bilocal $(\Delta S=1)^2$ aspect. The motivation to consider such diagrams stems from the importance of the single penguin diagram |8| (fig. 2) for the $K^o \to 2\pi$ decay.

The experience gained in our previous applications of penguin loops |9| enables us to estimate the three-loop double penguin diagrams. In this paper, therefore,

we first outline the simplified treatment of the double penguin performed in ref. [5], and then proceed to a presentation of a more rigorous approach:

(i) We improve the loop calculation by keeping the momentum dependence of the penguin loop and the "non-leading" terms.

(ii) We take into account the non-local part of the single penguin loop.

(iii) We take into account the crossed diagrams, which cannot be given a LD interpretation.

The new physical ingredients (i) to (iii) appear to be necessary in order to draw reliable conclusions about the role of double penguin diagrams.

2. Constant versus momentum-dependent penguin loop. Let us first rederive the conditions used by Hochenberg and Sachs [5] and then gradually improve the treatment, as stated above. Up to Dirac spinors and γ matrices, the single penguin has the formal structure [5]

$$P = \alpha_s\{\lambda_u L_u + \lambda_c L_c + \lambda_t L_t\} , \tag{1a}$$

where

$$L_q \equiv \ln \frac{M_w^2}{m_q^2} \tag{1b}$$

represents the result for the hard quark loop momenta p in the region $m_q^2 < p^2 < M_w^2$. Since the Kobayashi-Maskawa (KM) factors are constrained by the relation

$$\lambda_u + \lambda_c + \lambda_t = 0 , \tag{2}$$

eqs. (1) can be cast into the form

$$P(\mu^2) = \alpha_s(\lambda_u \ln \frac{m_c^2}{\mu^2} - \lambda_t \ln \frac{m_t^2}{m_c^2}) \quad , \tag{3a}$$

exhibiting the generalized GIM mechanism. The top-quark mass appears to be the highest loop momentum contributing to P, and m_u is replaced by the renormalization point $\mu \lesssim 1$ GeV. The KM factors of interest are

$$\lambda_u = V_{ud}V_{us}^* \quad \text{and} \quad \lambda_t = V_{td}V_{ts}^* \ . \tag{3b}$$

Then the procedure of Hochenberg and Sachs |5| consists in taking (3a), fixed at the hadronic scale μ, as an effective vertex appearing in fig. 3. Taking the top-quark mass as a common cut-off for the loop integral |4,10| of fig. 3

$$\int \frac{d^4p}{(2\pi)^4} \left(\frac{\not p}{p^2}\right)^2 [P(p^2)]^2 + \frac{\pi^2}{16} [P(\mu^2)]^2 \int^{m_t^2} dp^2 = m_t^2 \left[\frac{\pi P(\mu^2)}{4}\right]^2 \tag{4}$$

results in formula (25) of ref. |5|. However, we disagree with the procedure in (4) (performed under the assumptions of the constant momentum-independent P and m_t as a common cut-off). Actually, m_t is the effective cut-off only for the term $\sim\lambda_t$ in (3a), the cut-off for the second term $\sim\lambda_u$ being given by m_c. In the leading logarithm approximation there are more appropriate expressions for the effective vertices in fig. 3:

$$P(p^2) = \begin{cases} \lambda_u \alpha_s(p^2) \ln \dfrac{m_c^2}{p^2} \ , & \mu^2 < p^2 < m_c^2 \ , \\ \lambda_t \alpha_s(p^2) \ln \dfrac{m_t^2}{p^2} \ , & m_c^2 < p^2 < m_t^2 \ . \end{cases} \tag{5}$$

Accordingly, the result in (4) should be replaced by

$$\frac{\pi^2}{16} [\lambda_u^2 I(\mu^2, m_c^2) + \lambda_t^2 I(m_c^2, m_t^2)] \ , \tag{6a}$$

where

$$I(m^2,M^2) \equiv \int_{m^2}^{M^2} dp^2 \left[\alpha_s(p^2) \ln \frac{M^2}{p^2}\right]^2 . \qquad (6b)$$

The dominant contributions to the type of integrals appearing in (6) normally come from the upper parts of the integration regions. The integrals in (6), however, cannot be estimated by inserting the upper limit of integration, since these would vanish because of the logarithms. Moreover, we cannot use the "logarithmic integration" |10,11| and we therefore perform the integration numerically |11|.

For quark loops renormalized at $p^2 < M^2$, the $\alpha_s(p^2)$ to be used in (7) is

$$\alpha_s(p^2) = \frac{\alpha_s(M^2)}{1 - b \frac{\alpha_s(M^2)}{4\pi} \ln \frac{M^2}{p^2}} , \qquad (7)$$

where $b = 11 - \frac{2}{3} N_f$, N_f being the effective number of flavours. We take the numerical values $m_c = 1.4$ GeV and $m_t = 45$ GeV, and a few choices of the scale μ: (a) $\mu = 0.5$ GeV, (b) $\mu = 0.7$ GeV and (c) $\mu = 1$ GeV, at which $\alpha_s(\mu^2) = 1$.

Note that the leading log approximation (5) gives no interference term $\sim\lambda_u\lambda_t$ in (6a) because the logarithms $\ln m_c^2/p^2$ and $\ln m_t^2/p^2$ have no common loop momentum. For convenience, we define a dimensionless quantity $\hat{I}(m^2,M^2)$ by

$$I(m^2,M^2) = \left[M\alpha_s(M^2)\right]^2 \hat{I}(m^2,M^2) . \qquad (8)$$

We display the values for the integrals $\hat{I}$ in the "leading log" columns of table 1. Since $(\alpha_s(m_c^2))^2\hat{I}(\mu^2,m_c^2)$ and

$(\alpha_s(m_t^2))^2\hat{I}(m_c^2,m_t^2)$ are roughly of the same order of magnitude, m_t^2 is not the effective cut-off for the term $\sim\lambda_u$ containing u and c quarks in the single penguin loop.

The leading log approximations (5) are acceptable for the single-loop penguin diagram as long as $p^2 << m_c$ and $p^2 << m_t^2$, respectively. These restrictions in p^2 are not valid when the individual penguins are inserted into our three-loop diagram. Therefore, $\ln M^2/p^2$ has to be replaced by the full expression [9,11]

$$C(p^2,m^2,M^2) = 6\int_0^1 dx\, x(1-x)\, \ln\frac{M^2+p^2x(1-x)}{m^2+p^2x(1-x)} . \qquad (9)$$

This replacement substantially changes the integrals $\hat{I}$ in table 1. In addition, there is a non-zero interference term $\hat{K} \sim 2\lambda_u\lambda_t$ in the expression

$$\frac{\pi^2}{16}\left[\lambda_u^2 I(\mu^2,m_c^2) - 2\lambda_u\lambda_t K(\mu^2,m_t^2) + \lambda_t^2 I(m_c^2,m_t^2)\right] , \qquad (10a)$$

which replaces eq. (6a). Similarly to (8), we define $\hat{K}$ by

$$K(\mu^2,m_t^2) = \int_{\mu^2}^{m_t^2} dp^2\left[\alpha_s(p^2)\right]^2 C(p^2,m_u^2,m_c^2)C(p^2,m_c^2,m_t^2)$$
$$\equiv \left[m_t\alpha_s(m_t^2)\right]^2 \hat{K}(\mu^2,m_t^2) . \qquad (10b)$$

The values for the integrals $\hat{I}$ and $\hat{K}$ obtained by using the full expression (9) are displayed in the "full" columns of table 1.

3. Effects of the non-local part of penguin diagrams and a set of double penguin diagrams. In considering the diagram shown in fig. 1a, we have taken into account only the "local" part of the penguin. In fact, the single-loop penguin diagram

for the s → dG transition (fig. 2) has the following form in momentum space (KM factors omitted) |9|:

$$\left[\frac{g_s}{4\pi^2}\sqrt{2}\,G_F\,\frac{1}{6}\,C(p^2,m^2,M^2)\right]\bar{d}\,\gamma_\alpha\lambda^a\,L s\,P_{T_p}^{\alpha}(p)\ , \qquad (11)$$

where $m = m_u$, $M = m_c$ or $m = m_c$, $M = m_t$. In double-penguin diagrams, the transverse projector P_T becomes accompanied by the gluon propagator $D_G^{\rho\beta}(p) = \frac{1}{p^2}\left[g^{\rho\beta}-(1-\xi)\,\frac{p^\rho p^\beta}{p^2}\right]$ in such a way that the product is gauge-independent:

$$P_{T_p}^{\alpha}(p)\;D_G^{\rho\beta}(p) = g^{\alpha\beta} - \frac{p^\alpha p^\beta}{p^2}\ . \qquad (12)$$

We refer to the first and second term on the right-hand side of (12) as to the "local" (ℓ) and "non-local" (n) contribution of the penguin, respectively. The part $\sim g^{\alpha\beta}$ in (12) reduces to the truly local penguin operator |9| if all external quark momenta and the gluon momentum are $\sim M$. The terms coming from the "non-local" part $\sim (p^\alpha p^\beta)/p^2$ in (12) cannot be neglected when some of the gluon and quark momenta are far off-shell, as they are when the penguin loop is inserted in a higher loop diagram |9|.

With use of expressions (11) and (12), the purely local part of the diagram in fig. 1a can be written as

$$M_a(\ell\times\ell) = \left(\frac{g_s}{2}\right)^2(\bar{d}\,\gamma^\sigma L\lambda^a\lambda^b s)(\bar{d}\,\gamma_\sigma L\lambda^b\lambda^a s)\tilde{L}\ , \qquad (13)$$

where the loop integral is given by (masses are as stated below (11))

$$\tilde{L} = \frac{1}{36}\int\frac{d^4p}{(2\pi)^4}\,\frac{1}{p^2}\,C(p^2,m_1^2,M_1^2)C(p^2,m_2^2,M_2^2)\ . \qquad (14)$$

A method for evaluating this integral has already been presented in the preceding section, and the results

obtained are listed in table 1.

Invoking the "non-local" part of the penguin, we obtain for the total amplitude of diagram 1a

$$M_a = M_a(\ell\times\ell) - M_a(\ell\times n) - M_a(n\times\ell) + M_a(n\times n) \ . \qquad (15)$$

After some manipulations (using $p_\alpha p_\beta \to \frac{1}{4} g_{\alpha\beta} p^2$, etc. and the γ-matrix algebra), eq. (15) takes the form

$$M_a = -\frac{3}{4} M_a(\ell\times\ell) \ . \qquad (16)$$

Each of the four diagrams in fig. 1 can be treated in a similar way.

The crossed diagram 1b, when compared with eqs. (13) and (16), has a slightly different overall factor and colour structure:

$$M_b = -\frac{9}{4} \left(\frac{g_s}{2}\right)^2 (\bar{d}\ \gamma^\sigma L\lambda^a\lambda^b s)(\bar{d}\ \gamma_\sigma L\lambda^a\lambda^b s)\ \tilde{L} \ . \qquad (17)$$

The amplitudes corresponding to the remaining two diagrams are given by

$$M_c = M_a \ , \quad M_d = M_b \ . \qquad (18)$$

Extracting the colour factors for the meson $\to$ meson transition, we find that the total amplitude is

$$M_a + M_b + M_c + M_d = -5\,\frac{16}{3}\,\tilde{M} \ , \qquad (19)$$

where

$$\tilde{M} \equiv \left(\frac{g_s}{2}\right)^2 (\bar{d}\ \gamma^\sigma L\ s)(\bar{d}\ \gamma_\sigma L\ s)\tilde{L} \ . \qquad (20)$$

Compare (19) with the purely local part of fig. 1a treated previously [5]:

$$M_a^{\mathrm{IIS}}(\ell\times\ell) = \left(\frac{16}{3}\right)^2 \tilde{M} \ . \qquad (21)$$

The effective difference in sign is obvious before we compare our calculation of the loop (in $\tilde{M}$) with that of ref. |5|.

4. Discussion and conclusion. In this paper we have treated three-loop double penguin diagrams. We have considered them as another short-distance ($\Delta S=2$) mechanism for the $K^0-\overline{K^0}$ mixing. This allows us to reconsider the extraction of the bound on m_t in the framework of the six-quark model. Let us emphasize that, similarly to the extraction of m_c in the four-quark model, such a procedure is limited because of an unknown long-distance contribution. In this paper we have shown that such extraction of m_t is not possible even if the neglect of long-distance contributions is valid. The reason for this is twofold: (i) The numerical value of the *SD* double-penguin loop contribution is negligible in comparison with the estimate of ref. |5|. (ii) The sign of the contribution is changed because of the "non-local" terms and crossed diagrams.

In order to draw a conclusion about the possible physical relevance of the double penguin, let us compare the three terms appearing in (10a). Their absolute magnitudes can be estimated by using the well-known value $|\lambda_u| = 0.21$ |12| and two different pieces of information, $|\lambda_t| \in (0.9\times10^{-4}, 2\times10^{-3})$ |13| and $|\lambda_t| < (1.15\times10^{-3}, 2.6\times10^{-3})$ |14|. This gives a rough estimate of the absolute values

$$|\lambda_u|^2 I(m^2, m_c^2) \sim 10^{-1} >> 2|\lambda_u||\lambda_t| K(\mu^2, m_t^2) \sim 10^{-3} >> |\lambda_t|^2 I(m_c^2, m_t^2) \sim 10^{-5} . \qquad (22)$$

Then the first term $\sim\lambda_u^2$ in (10a), being real, represents the main contribution to the K_L-K_S mass difference Δm. Comparison with the standard box value gives the SD ratio $\Delta m^{(\text{double penguin})}/\Delta m_{(\text{box})} \sim 10^{-2}$, which is to be contrasted with the value 10 or more by Hochenberg and Sachs [5]. We obtain approximately the same value, $\sim 10^{-2}$, for the ratio of the imaginary part of the double penguin (represented mainly by the interference term $\sim\lambda_u\lambda_t$ in (10a)) to the imaginary part of the standard box. This also shows that the CP-violating part of the SD double penguin amplitude in the previous paper [5] was overestimated by three orders of magnitude.

However, there may exist diagrams other than double-penguin, which may turn out to be physically relevant. For example, there is a diagram (fig. 4) of the same order in the coupling constants as the double penguin, which corresponds to a photopenguin diagram [9] considered in our previous treatment of CP violation (via the neutron electric dipole moment). In the latter case, such photopenguin contributions turn out to be larger than the penguin contributions by a factor of 20-50. A more complete investigation of the CP-violating parameter ϵ, including the contribution from the diagram in fig. 4, will be considered in more detail elsewhere.

In addition, although the SD double penguins appear to be physically irrelevant, the complementary LD $(\Delta S=1)^2$ double penguins [6,7] might still be important.

We thank G.Ecker for useful comments

References

|1| S.L. Glashow, J. Iliopoulos and L. Maiani, Phys. Rev. D2 (1970) 1285.

|2| M.K. Gaillard and B.W. Lee, Phys. Rev. D10 (1974) 897.

|3| J. Ellis, M.K. Gaillard and D.V. Nanopoulos, Nucl. Phys. B109 (1976) 213;
A.J. Buras, Phys. Rev. Lett. 46 (1981) 1354;
T. Inami and C.S. Lim, Prog. Theor. Phys. 65 (1981) 297.

|4| L.B. Okun', Leptony i kvarki (Nauka, Moscow, 1981), Leptons and quarks (North-Holland, Amsterdam, 1982).

|5| D. Hochenberg and R.G. Sachs, Phys. Rev. D27 (1983) 606.

|6| C.T. Hill, Phys. Lett. 97B (1980) 275.

|7| G. Ecker, Phys. Lett. 147B (1984) 369.

|8| M.A. Shifman, A.I. Vainshtein and V.I. Zakharov, Nucl. Phys. B120 (1977) 316; ZhETF (USSR) 22 (1975) 123 [JETP (Sov. Phys.) 22 (1975) 55]; ZhETF (USSR) 72 (1977) 72 [JETP (Sov. Phys.) 45 (1977) 670].

|9| J.O. Eeg and I. Picek, Nucl. Phys. B244 (1984) 77; Phys. Lett. 130B (1983) 308.

|10| A.I. Vainshtein, V.I. Zakharov, V.A. Novikov and M.A. Shifman, Yad. Fiz. 23 (1976) 1024 [Sov.J.Nucl. Phys. 23 (1976) 540] ; Phys. Rev. D16 (1977) 223.

|11| J.O. Eeg, Phys. Rev. D23 (1981) 2596.

|12| Particle Data group.

|13| X-Y Pham and X-C Vu, LPTHE 83/28

|14| L-L Chau and W-Y Keung, Phys. Rev. Lett. 53 (1984) 1802.

Table 1

Numerical values for the loop integrals in eqs. (6), (8) and (10).

μ (GeV)	(u-c) loop, $\hat{I}(\mu^2, m_c^2)$		(c,t) loop, $\hat{I}(m_c^2, m_t^2)$		Interference term $\hat{K}(\mu^2, m_t^2)$	
	"l-log"	"full"	"l-log"	"full"	"l-log"	"full"
0.5	2.07	13.43	3.89	12.29	-	0.40
0.7	0.81	8.78	4.19	12.72	-	0.41
1	0.11	3.93	4.91	13.46	-	0.38

Figure captions

Fig. 1. Double penguin box diagrams for the K^{O}-$\overline{K^{O}}$ mixing.

Fig. 2. Penguin diagram for the $s \to dG$ transition.

Fig. 3. Double penguin in terms of the effective penguin vertices P and the light quarks q in the box loop.

Fig. 4. Example of a new contribution to the K^{O}-$\overline{K^{O}}$ mixing.

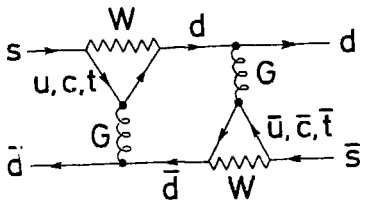

(a)

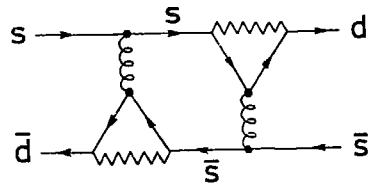

(c)

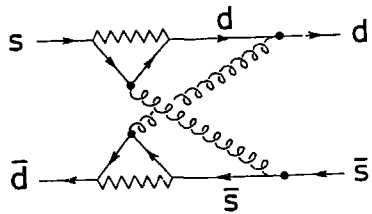

(b)

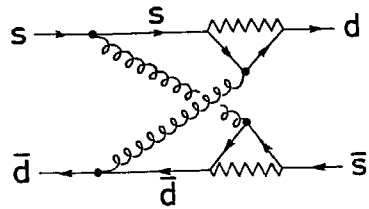

(d)

FIG. 1

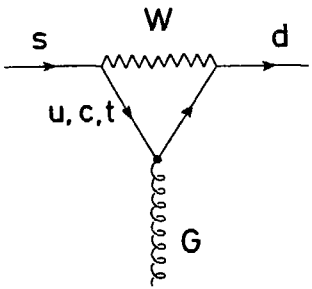

FIG. _

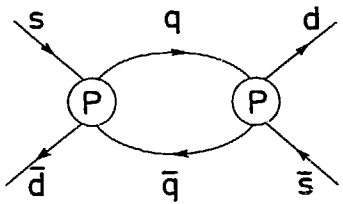

FIG. 3

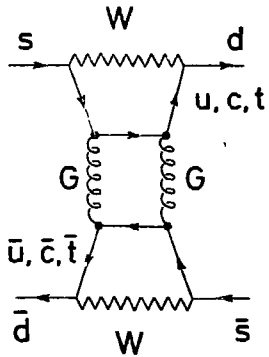

FIG. 4